ANALYSIS AND DESIGN OF A ZERO VOLTAGE TRANSITION DC-DC BOOST CONVERTER FOR PHOTOVOLTAIC (PV) ENERGY SYSTEM

A THESIS SUBMITTED IN PARTIAL FULFILMENTS OF THE REQUIREMENTS FOR THE AWARD OF THE DEGREE OF

Master of Technology
in
Industrial Electronics
Department of Electrical Engineering

By

VEMULA ANUSHA

Roll No: 212EE5259

Under the Guidance of

Dr. MONALISA PATTNAIK

Dr. B. CHITTI BABU

Department of Electrical Engineering

National Institute Technology, Rourkela-769008

NATIONAL INSTITUTE OF TECHNOLOGY

ROURKELA

CERTIFICATE

This is to certify that the project entitled "**ANALYSIS AND DESIGN OF A ZERO VOLTAGE TRANSITION DC-DC BOOST CONVERTER FOR PHOTOVOLTAIC (PV) ENERGY SYSTEM**" submitted by Vemula Anusha (212ee5259) in partial fulfillment of the requirements for the award of Master of Technology degree in Industrial Electronics, Department of Electrical Engineering at National Institute of Technology, Rourkela is an authentic work carried out by her under my supervision and guidance.

To the best of my knowledge the matter embodied in this thesis has not been submitted to any other university/Institute for the award of any Degree.

Date:

Place: Rourkela

(Dr. Monalisa Pattnaik)
Department of Electrical Engineering
NIT Rourkela

ACKNOWLEDGEMENT

On the submission of my thesis entitled "**Analysis and Design of a Zero Voltage Transition DC-DC Boost Converter for PV Energy System**" I would like to extend my gratitude and sincere thanks to my supervisor **Dr. Monalisa Pattnaik**, Asst. professor, Dept. of Electrical Engineering for her constant motivation and support during the course work. I am very thankful to her for giving me good basics in PV during the course work, which makes a good part of the project.

I am sincerely thankful to **Dr. B. Chitti Babu**, for helping me give a good start for the work. I truly appreciate and value his esteemed guidance and encouragement in the beginning.

I would like to thank all others who have consistently encouraged and gave me moral support, without whose help it would be difficult to finish this project.

I would like to thank my parents and friends for their consistent support throughout.

ABSTRACT

India being the world's third largest power producer and consumer is still considered to have unreliable electrical infrastructure. It is estimated that about 27% of the energy generated is stolen or lost in transmission. During the 2012 grid failure, some villages that were not connected to grid were not affected, such as Meerwada located in Madhya Pradesh because it has a 14KW solar power station. The photovoltaic (PV) energy systems are gaining popularity because the systems are being developed and designed to extract maximum energy from the sun in most efficient way and feed it to the loads without affecting their performance.

In this thesis, a boost converter operating all the switching devices under Zero Voltage Transition is studied and a model converter which can supply a load of 250W is designed and is used in a PV energy system. In this converter topology, a part of the circuit resonates for a small portion of the switching cycle of the converter, known as the auxiliary circuit that enhances the soft transition from ON state to OFF state and vice versa, thus improving the converter efficiency by reducing the dominating portion of in losses i.e. the losses that occur due to hard transition of the switches. Due to reduced losses during switching transitions heating effect of MOSFETs is reduced and they have a longer life. The comparative study between the new topology and conventional hard switching converter is analyzed in terms of improvement of efficiency and reduction of switching losses.

INDEX

CHAPTER-3

ZVT DC-DC BOOST CONVERTER

CHAPTER-4

PHOTO VOLTAIC ARRAY

CHAPTER-5

MAXIMUM POWER POINT TRACKING

CHAPTER-6

RESULTS AND DISCUSSION

REFERENCES

LIST OF TABLES

LIST OF FIGURES

LIST OF ABBREVIATIONS

PV	Photo Voltaic
ZVT	Zero Voltage Transition
DC	Direct Current
MOSFET	Metal Oxide Semiconductor Field Effect transistor
PWM	Pulse Width Modulation
EMI	Electro-Magnetic Interference
ZVS	Zero Voltage Switching
ZCS	Zero Current Switching
MATLAB	MATrix LABoratory
MPPT	Maximum Power Point Tracking
P&O	Perturb and Observe
IC	Incremental Conductance

LIST OF SYMBOLS

C_S	Snubber capacitance
V_{GS}	Gate to source voltage of the MOSFET
V_{DS}	Drain to Source voltage
I_D	Drain current
T_{on}	Turn-ON time of the MOSFET
T_{off}	Turn-OFF time of the MOSFET
P_{SW}	Switching Power losses
V_S	Voltage blocked by the switch
I_S	Flow of current allowed by the switch
f_S	Switching frequency of the converter
V_{in}	Input voltage
S_1	Main switch/boost switch
S_2	Auxiliary switch
L_{in}	Input boost inductor
L_r	Auxiliary resonant inductor
C_r	Auxiliary resonant capacitor
C_b	Energy feed forward capacitor
C_s	Parasitic capacitance of the switch
D_1-D_5	Diodes
C_0	Output capacitor
t_0-t_7	Time instants in one switching cycle
I_{Lr}	Current flowing through the auxiliary circuit

V_{cr}	Voltage blocked by the resonant capacitor
V_{cb}	Voltage blocked by the feed forward capacitor
P_{out}	Output power rating
V_{out}	Output voltage rating
V_{rp}	Output voltage ripple
ΔI_{rp}	Input peak current ripple
η	Efficiency of the converter
I_{in_pk}	Input peak current
D	Duty cycle
f_r	resonant frequency
V_b	Base voltage
I_b	Base current
Z_r	Resonant impedance
Z_{r_pu}	Per unit resonant impedance
Z_{rb}	Base resonant impedance
T_r	Resonating time period of the auxiliary circuit
t_{rr}	Reverse recovery time of the diode in the boost circuit
V_{S2_pk}	Peak voltage across S_2
K	constant
I_{S2_pk}	Peak current of S_2
I_{S2_rms}	RMS current of S_2
I_{S1_rms}	RMS current of S_1
I_{PV}	PV current
I_0	Diode's reverse saturation current
V_T	Diode's thermal voltage

a	Diode's ideality factor
K_I	Temperature coefficient of I_{sc}
K_V	Temperature coefficient of V_{oc}
G	Irradiance on the surface of the cell
G_{STC}	Irradiance under STC
I_{PV_STC}	Photocurrent generated under Standard Test Conditions (STC)
E_g	Energy gap of the semiconductor
I_{0_STC}	Nominal saturation current
I_{SC_STC}	Nominal value of I_{sc}
V_{OC_STC}	Nominal value of V_{oc}
N_s	Number of modules in a serial connected string
N_p	Number of strings that are connected in parallel
V_{mp}	Operating Voltage at MPP
I_{mp}	Operating Current at MPP
P_{max}	Maximum power

CHAPTER-1

1.1 INTRODUCTION

Usually, the converters operating under Zero Voltage Transition (ZVT) help solving the problem of prohibitive Electromagnetic Interference (EMI) either by using a diode whose recovery characteristics are not fast, to increase the turn OFF time switch present in the boost circuit, which increases the switching losses [3], or by using passive snubber circuits which increase the conduction losses [4] [5], thus reducing the converter efficiency and limiting the switching frequency. So the problem of EMI is solved only at the cost of reduced efficiency. So there is a need for highly efficient converters with reduced EMI.

The most important thing in the converter design is the positioning of the auxiliary switch. If the source terminal of the switching MOSFET is not connected to the common point of grounding in the circuit, we will need a floating gate drive, which demands an effective gate voltage greater than the input voltage. A reduced stress of voltage and current peaks on the switching devices is always recommended for safety of devices.

The principle of ZVT is that the auxiliary circuit carries a current higher than the input current flowing through the boost inductor just for a fractional part of switching time, in order to attain soft turn ON and OFF transitions of the main and auxiliary switches. So, these converters have higher ohmic losses than the simple or conventional converters that do not operate under soft transitions of switching. But the efficiency of the soft switching converters is high as the losses due to hard switching in the soft switching converters are very low as compared to the conventional hard switching converters. Also, as the auxiliary circuit it-self is soft switching and due to the creative placing of the snubber capacitor which controls the ON to OFF transition of the switch in the boost circuit, this converter reduces the EMI and increases the efficiency.

1.2 LITERATURE REVIEW

In conventional hard switching converters, the conduction losses are very low. But due to high switching losses, the efficiency of these converters is low. So the technique of soft switching is introduced to make the switching transitions at either zero voltage condition or zero current condition, so that the dominating portion of losses (the ones caused due to switching under high voltages or currents) can also be reduced and the efficiency of the converters can be highly improved.

In [3] it has been made clear that the sources of major losses in a boost converter operating in CCM are the diode and the inductor present in the part of the circuit that boosts the voltage and the MOSFET used for switching. The efficiency is also affected by the input boost inductor's refined design and the OFF transition losses of the main switch. As the turn ON losses of the switch depend on the reverse recovery characteristics of the diode in the boost circuit, adopting a fast recovery diode reduces the turn-ON losses. But, use of a fast recovery diode increases ringing effect and EMI. Further we need to use EMI filters which would increase the complexity and may affect the improvement in efficiency achieved by using fast recovery diode.

In [4] the process of active turn-ON snubbing for the ZVT is studied. The use of an extra switch to make easy discharge of resonant inductor to reduce voltage stress on main switch is an alternative for passive snubbing. This configuration of active snubbing is usually referred to as the ZVT boost converter. This paper has provided the basic idea of the implementing boost converter with zero voltage transitions. But in this circuit only the boost circuit switch operates in zero voltage transitions. But the auxiliary circuit switch operates on zero current transitions. The resonant energy that has been stored in the inductance of the resonating circuit is circulated to the load.

Many papers have been referred only to study the different methods adopted in the turn-off process of the boost switch present in the main circuit. In [2] the snubber capacitance C_s controls turns off process of the boost switch by controlling the rate of rise of voltage across the switch. But the energy that has been stored in this capacitor is always dissipated in the auxiliary circuit. This increased the conduction losses of the converter. In [5] the conduction losses are

slightly reduced by using an energy feed-forward circuit. In this circuit, some part of the resonant energy is allowed to be directly fed to the connected load by making use of a transformer. The circuit topology presented in this thesis has all its resonant energy dissipated into the load.

1.3 MOTIVATION

In recent days of continuously and rapidly growing power demand and but very slowly improving supplying capacity, there are more chances of power outage or grid failures like in the case of 2012 grid failure in India. Also most of the remote areas are not connected to the grid and they do not have power supply. These areas can generate power on their own using renewable resources such as solar energy.

The efficiency of the PV energy system solely depends on the PV panels, power converter and the Maximum Power Point Tracking system. The efficiency of a single PV cell is very low. The efficiency of hard switching converters is low. So they can be replaced by the soft switching converters that have very less losses and high efficiency. Use of good and efficient MPPT algorithm also improves the system efficiency. In this thesis, improvement of converter efficiency is most focused on.

Usually ZVT converters solve the problem of EMI either by using slow recovery diodes or by using passive snubbers which increase the conduction losses. So the reduction of EMI is achieved only at the cost of reduced efficiency. So there is a need for more efficient converters with less EMI. Also most of the soft switching converters involving auxiliary switch does not attain soft switching of the auxiliary switch. So an auxiliary circuit which helps in soft switching and also is soft switching is required.

1.4 OBJECTIVES

The main objective of this thesis is to study and analyze the operation of converter and design the converter that can satisfy all the requirements that have motivated to take up this work. In short the objectives of the thesis are listed as follows

1. To design a converter that has
    a. Reduced switching losses
    b. Reduced conduction losses
    c. Less EMI
    d. Reduced stress of voltage and current on the devices
2. Study the operation of the converter and verify it by waveforms and study the soft switching of both the switches.
3. Implementation in PV environment along with MPPT
4. Calculation of losses and efficiency of the converter and comparative study with a simple boost converter

CHAPTER-2

2.1 BOOST CONVERTER FOR PV ENERGY SYSTEM

The efficiency of a photovoltaic system is very low since the output of the PV array depends on various environmental conditions most likely to be temperature and solar irradiation. Therefore, there is a need for a system to condition the power output of the PV array before supplying it to the domestic loads.

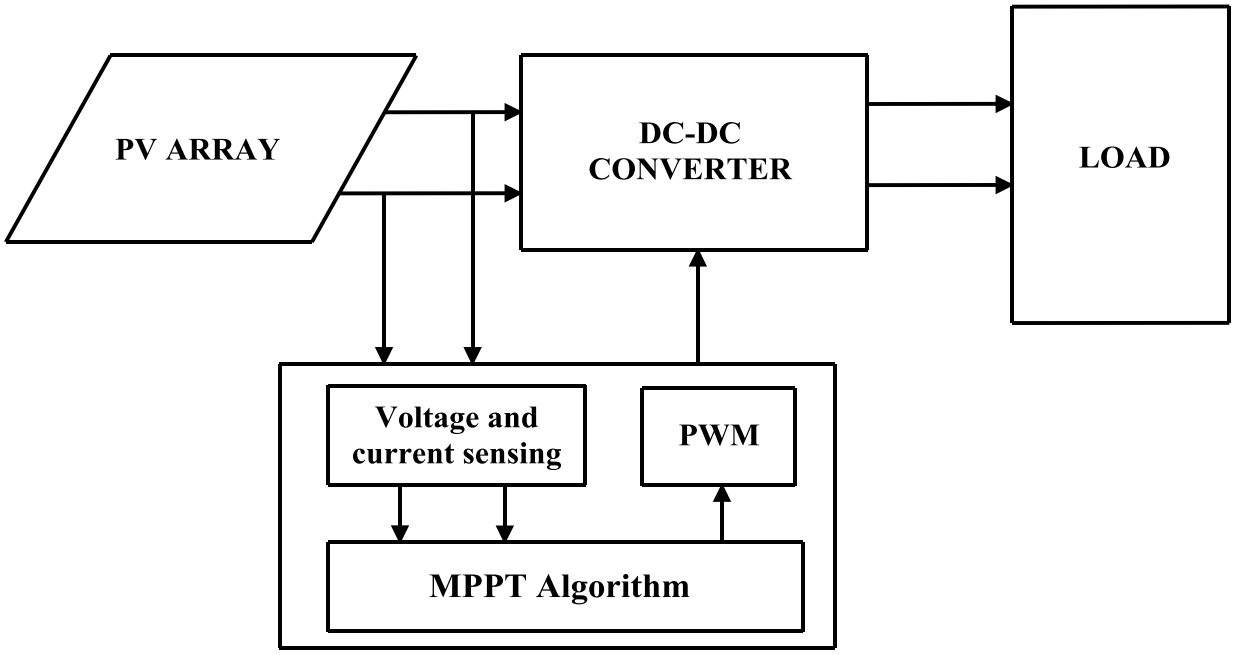

Figure 2.1: block diagram of DC-DC converter with PV energy system

Figure 2.1 represents a block diagram showing the use of a converter for PV energy system. The PV array's output is supplied to the load after being conditioned by the ZVT DC-DC boost converter. The switching of the MOSFETs constituting the circuit is controlled by a maximum power point tracking (MPPT) algorithm which tracks that operating point of the PV array that meets the DC load line (including the effect of converter).

2.2 POWER LOSSES IN HARD-SWITCHING CONVERTERS

In the switching converters, when the switching device is in ON state, as the voltage blocked by the switch is zero, the power losses are zero. When the switch remains in the off state, as the current allowed by the switch is zero, the power losses are zero. But during the transition of the switch from both ON state to OFF state and OFF state to ON state, if there is no mechanism to make either voltage or current zero, power losses occur. This is in the case of hard-switching converters.

In the hard switching converters, power losses will occur when there will be a simultaneous non-zero voltage applied across and non-zero current flowing through the switch. When the switching device turns ON or OFF, the device voltage and current are high in simultaneous cases resulting in high losses. This is shown as waveforms in figure 2.2, (i) showing control pulse given to the switching device, (ii) the device voltage and current and (iii) power losses per switching cycle.

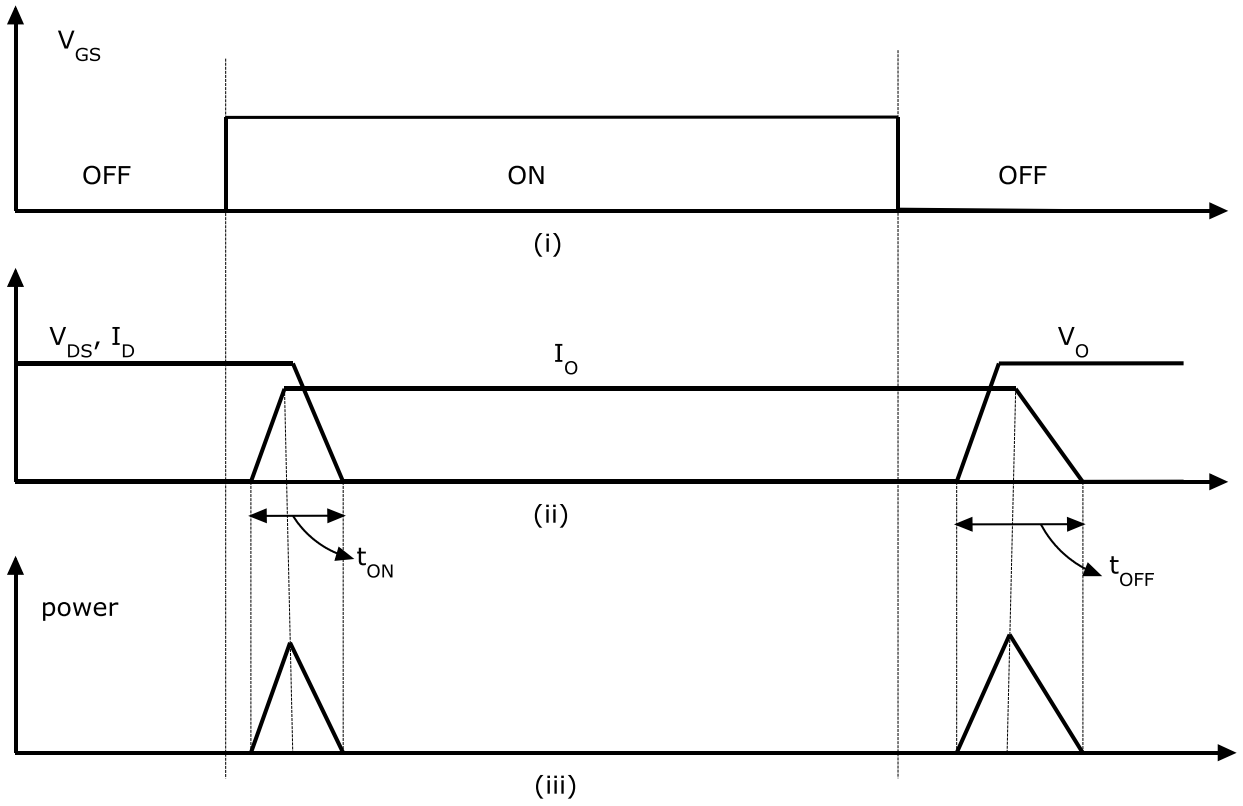

Figure 2.2: switching losses in hard switching converters

The power losses corresponding to a single switching transition are the product of the voltage that appears across the terminals of the switch and the current flowing through the switch. The entire switching losses are the product of energy or power lost per switching transition and the switching frequency. The power losses that occur due to these switching transitions are referred to as switching losses.

The switching losses in one switching cycle can be denoted in equation 2.1

$$P_{sw} = V_s I_s f_s \left(\frac{T_{on} + T_{off}}{2} \right) \tag{2.1}$$

From the above equation, the switching losses in any semiconductor device vary linearly with switching frequency and delay times. Therefore such hard switching converters cannot be used for high frequency switching applications. Though use of passive snubbers across the switch reduces voltage stresses, the efficiency cannot be improved due to high switching losses.

From the equation of switching losses, it can be observed that the switching losses can be reduced in 2 ways

i. By reducing the delay times during turn ON and turn OFF, by using faster and more efficient switches in converter.
ii. By making the voltage across or current through the switch zero before turning it ON/OFF, the concept of soft switching converters.

2.3 SOFT SWITCHING TECHNIQUES

There are two basic methods to attain soft switching, zero current switching (ZCS) and zero voltage switching (ZVS), based on the parameter that is made zero, either the voltage or current through the device.

2.3.1 ZERO CURRENT SWITCHING

A switch operating with ZCS has an inductor and a blocking diode in series with it. The switch turns ON under ZCS as the rate of rise of current after the voltage becomes zero is controlled by the inductor. As the inductor does not allow sudden change in current, it rises linearly from zero.

When a negative voltage is made to appear across the combination of inductor and switch using a resonant circuit, the current flowing through the switch is naturally reduced to zero which results in the turn OFF of the switch under zero current switching.

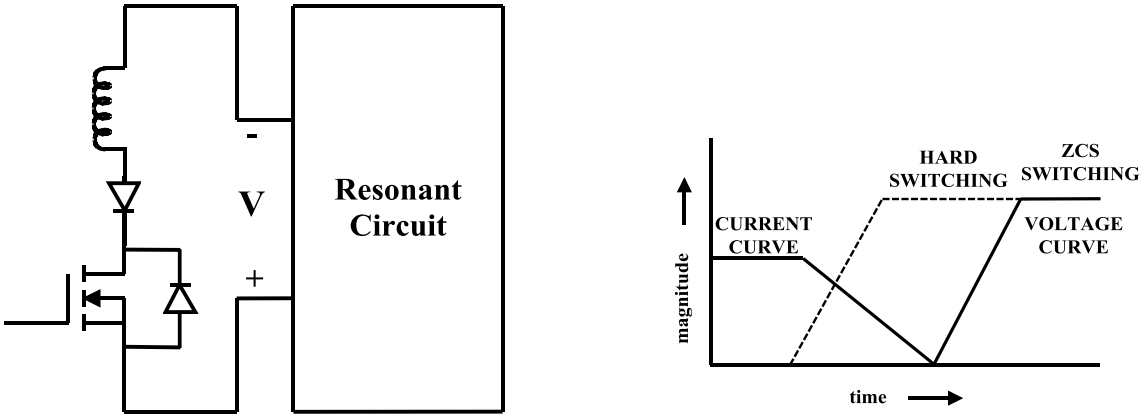

Figure 2.3: (a) ZCS turn OFF using negative voltage

(b) Switching waveforms of hard switching and ZCS during turn OFF

2.3.2 ZERO VOLTAGE SWITCHIING

A switch operating with ZVS has an anti-parallel diode and a capacitor across it. During turn OFF as the current reduces to zero, the rate of voltage rise that takes place across the switch is controlled by the capacitor. As the capacitor does not allow sudden change in voltage, it rises linearly from zero.

The turn OFF characteristics of the switch are controlled by a capacitor connected across it. This capacitor reduces the voltage rise rate as current flow reduces to zero.

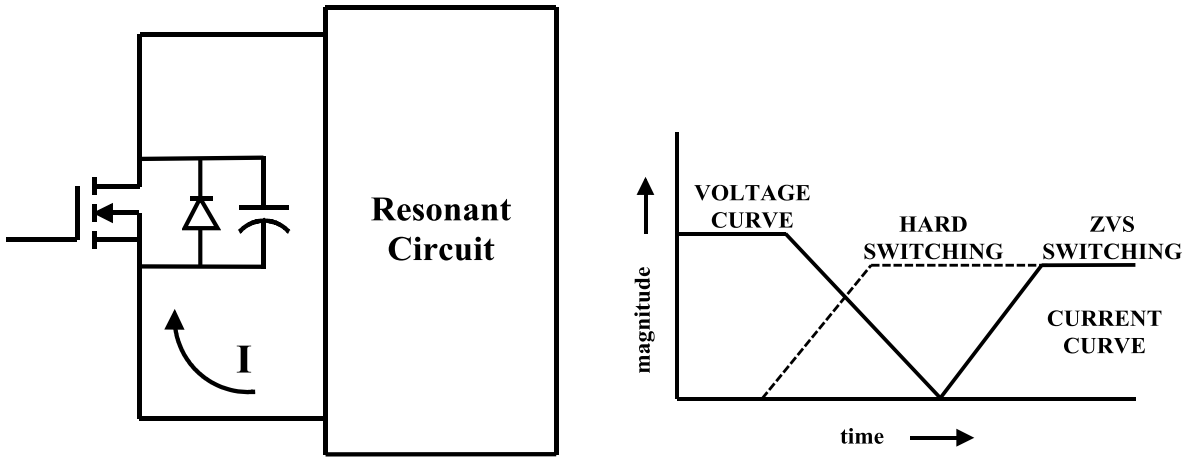

(a) (b)

Figure 2.4: (a) ZVS turn ON using negative current

(b) Switching waveforms of hard switching and soft switching

2.4 ZERO VOLTAGE TRANSITION CONVERTERS

The ZVT converters accomplish zero voltage switching during both turn-ON and turn-OFF transitions of the primary or boost switch.

The zero voltage transition in zero voltage switching converters is accomplished by turning OFF the switch which has capacitor and a diode connected in parallel with it. As the flow of current through the switch falls to zero, the capacitor maintains zero voltage across the switch. Where as in zero voltage transition, as the switch turns OFF, the current in the switch is transferred to the capacitor connected in parallel to it.

The turn ON transition in zero voltage switching is accomplished by discharging the capacitor connected in parallel by making use of the energy stored in a magnetic circuit

element like a transformer winding or an inductor coil. The switch is turned ON after the parallel diode enters into the state of conduction. This ensures a zero voltage across the switch during transition.

There are various zero voltage switching techniques. Each one differs from other in the techniques used to control and modulate to attain regulation and also in the mechanism of storing energy to attain zero voltage turn ON.

CHAPTER-3

ZERO VOLTAGE TRANSITION DC-DC BOOST CONVERTER

3.1 CIRCUIT DESCRIPTION AND ITS NOVELTY

The circuit schematic of the zero voltage transition DC-DC boost converter is shown in Figure 3.1. It is just a simple boost converter with a diode D_1, input boost inductor L_{in}, main switch S_1 and an output capacitor C_0 across a load $R_{load.}$ In addition to the boost circuit, it also constitutes of an additional circuit that resonates, consisting of an inductor L_r, a capacitor C_r, diodes D_2-D_5 and a capacitor C_b to feed the resonant energy to the load. The capacitance C_s shown across the main switch S_1 is its parasitic capacitance and not an external capacitance.

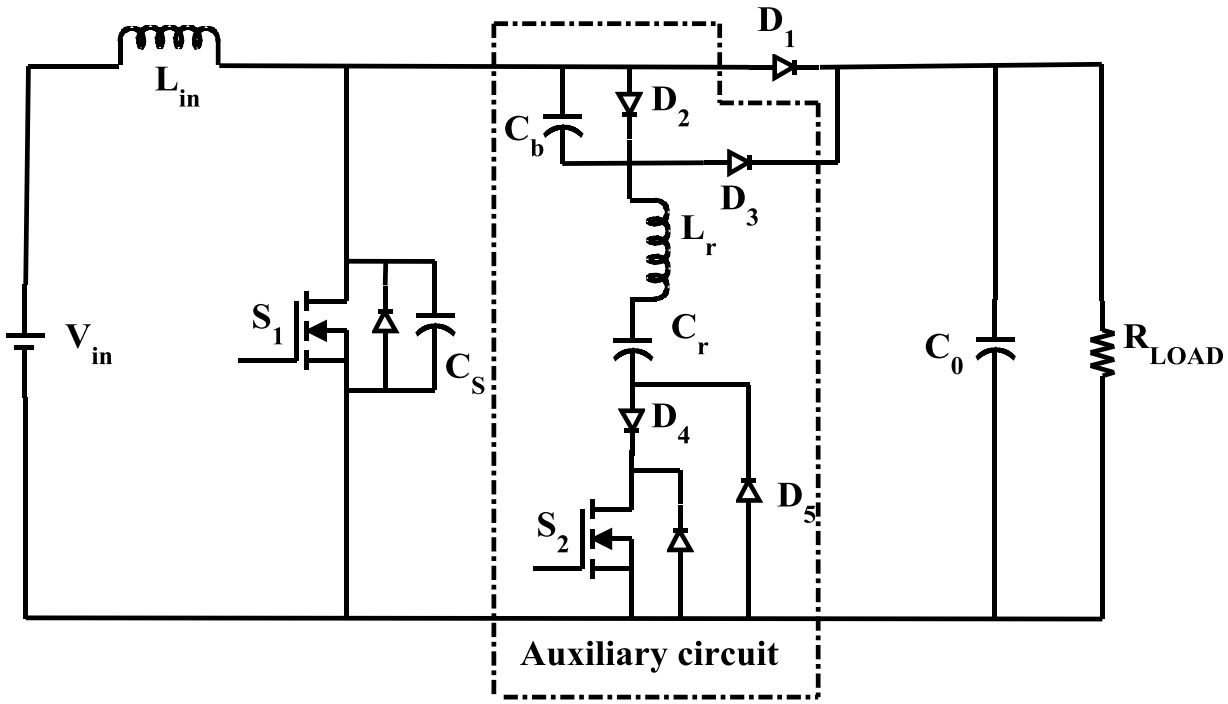

Figure 3.1: Schematic diagram of the ZVT dc-dc boost converter

The basic principle of Zero Voltage Transitions is that the auxiliary circuit carries a current higher than that of the input supply current, for a small portion of the entire switching cycle in order to attain soft switching of the switching elements present in the converter. Therefore Zero Voltage Transition converters have higher ohmic losses than that of those

converters that operate under hard-switching. But the efficiency of the converters that operate under soft switching is inflated unlike the hard switching converters on account of diminished switching losses.

The innovative part of this circuit lies in the reduction of conduction losses along with soft switching of all the switches main and the auxiliary ones, and also all the diodes. This is achieved by using a capacitor that controls the turn-off characteristics of the main switch, whose resonant energy all dissipated into the load. From figure 3.1 it is clear that the capacitor C_b is the feed-forward capacitor that controls the turn-off of the main/boost switch. The energy retained by this capacitor is completely discharged into the load through the boost diode, either D_1 or D_3. So the rms current carried by the auxiliary circuit is reduced and so happens with the conduction power losses, unlike the other topologies mentioned in the literature review.

3.2 CIRCUIT OPERATION

The operation of the circuit is explained for one complete switching cycle, which is split into seven parts for easy understanding. Each of these cases is explained along with equivalent circuit for that interval. Initially the boost diode D_1 supplies the output current and the circuit acts as a simple pulse width modulated boost converter. The circuit under this condition is shown in figure 3.2.

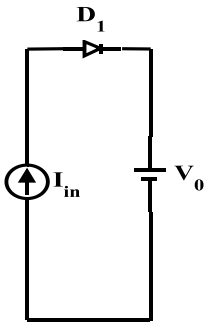

Figure 3.2: [$t<t_0$] converter circuit in simple boost converter mode

Interval 1 [t_0-t_1]:

At instant t_0 the switch S_2 is switched ON with Zero Current Transition owing to the existence of auxiliary resonant inductor serially connected to it. The current slowly starts to divert from the diode D_1 to that part of the circuit which supplements the main circuit, which eventually starts to resonate. The resonant inductor decelerates the turn-off current rate through D_1 that turns off under ZCS by the end of this interlude. By this time the auxiliary current flowing through boost inductor equals the input boost current. The equivalent circuit for this interval is manifested in figure 3.3.

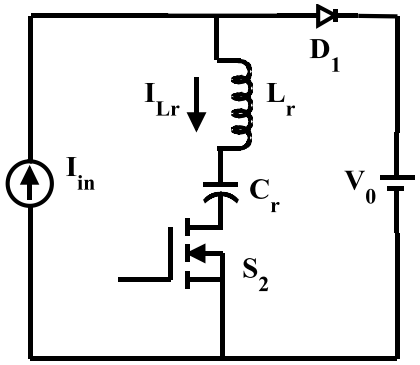

Figure 3.3: Equivalent circuit for interval [t_0-t_1]

Interval 2 [t_1-t_2]:

The auxiliary circuit current keeps on increasing all interval long. But the input current supplied is assumed to be constant due to large inductance which does not allow sudden change in current. So the parasitic capacitance C_s of the main switch S_1 starts discharging into the auxiliary circuit in order to supply the increased portion of auxiliary current. By the end of this interval the capacitance discharges completely. The equivalent circuit for this interval is manifested in figure 3.4.

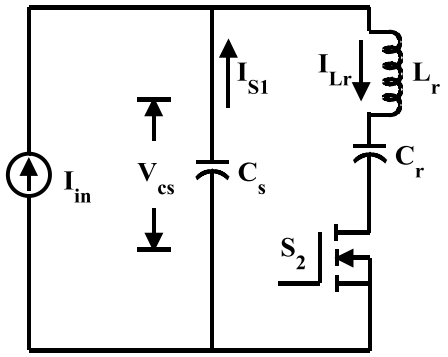

Figure 3.4: Equivalent circuit for interval [t_1-t_2]

Interval 3 [t_2-t_3]:

After the instant t_2 the diode internally present in the main switch connected anti parallel to it starts conducting, which causes the voltage blocked by the main switch S_1 to be zero. This is the Zero Voltage duration during which the switch S_1 must be supplied with the trigger. By the end of this interval the current carried by the auxiliary circuit equals the input supply current and the main switch is in a condition of about to start conduction. The equivalent circuit of the converter for this mode is manifested in figure 3.5.

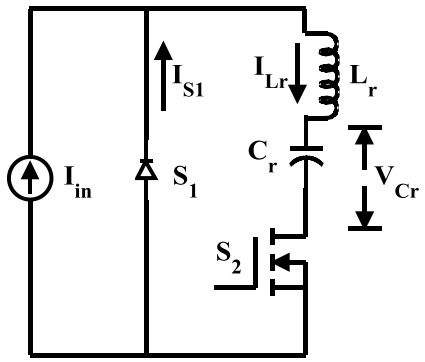

Figure 3.5: Equivalent circuit for interval [t_2-t_3]

Interval 4 [t_3-t_4]:

The auxiliary current declines the input supply current and the residue of the input supply current after supplying with the auxiliary current starts flowing through the switch S_1. By the end of this

interval the flow of current in the auxiliary circuit becomes zero. The equivalent circuit of the converter for this mode is manifested in figure 3.6.

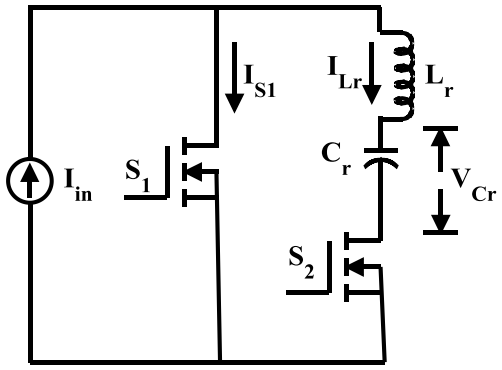

Figure 3.6: Equivalent circuit for interval [t_3-t_4]

Interval 5 [t_4-t_5]:

In this interval, the direction of current flow in the auxiliary part of the circuit changes and the negative portion of the resonant cycle starts at this instant. Diode D_4 which is in series the switch makes the branch unidirectional and does not allow the switch S_2 to conduct and so this current passes through the diode D_5 creating a Zero Voltage turn-off condition for S_2. Meanwhile the current from the diode D_2 is rerouted to the capacitor C_b which starts getting charged. The equivalent circuit for this interval is manifested in figure 3.7.

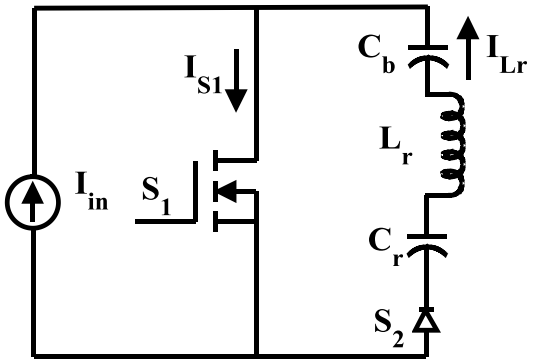

Figure 3.7: Equivalent circuit for interval [t_4-t_5]

Interval 6 [t_5-t_6]:

As this interval starts at instant t_5, the auxiliary current becomes zero and the resonant cycle ends here. The circuit begins to runs identical to a PWM boost converter operating in its charging state. The equivalent circuit of the converter in this interval is manifested in figure 3.8.

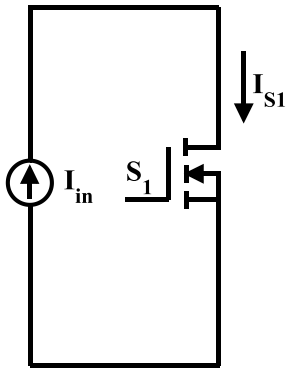

Figure 3.8: Equivalent circuit for interval [t_5-t_6]

Interval 7 [t_6-t_7]:

At the beginning of this interval at instant t_6 S_1 is turned-off. The feed forward capacitor C_b is responsible for the slow voltage rise across S_1. Voltage across the capacitor C_b reverse biases the boost diode D_1 and it cannot conduct. So the energy stored in the capacitor C_b during the resonant cycle i.e. the auxiliary circuit energy discharges through diode D_3 and when this voltage reaches zero the diode D_1 starts conducting and the succeeding switching cycle gets initiated. The equivalent circuit of the converter for this mode is shown in figure 3.9.

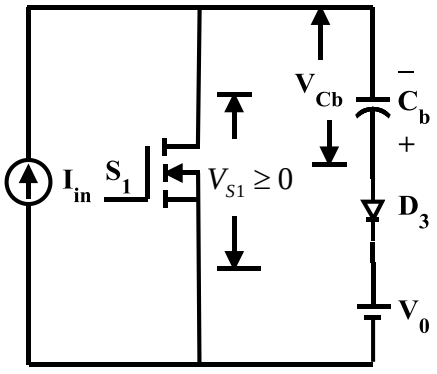

Figure 3.9: Equivalent circuit for interval [t_6-t_7]

3.3 THEORETICAL WAVEFORMS

Figure 3.10 shows the theoretical waveforms for the operation of the converter showing each interval in the entire switching cycle. The variations of the resonant circuit current and voltage of the inductor and capacitor respectively, switch voltages and currents (both main and auxiliary), the feed forward capacitor voltage in each interval are shown clearly.

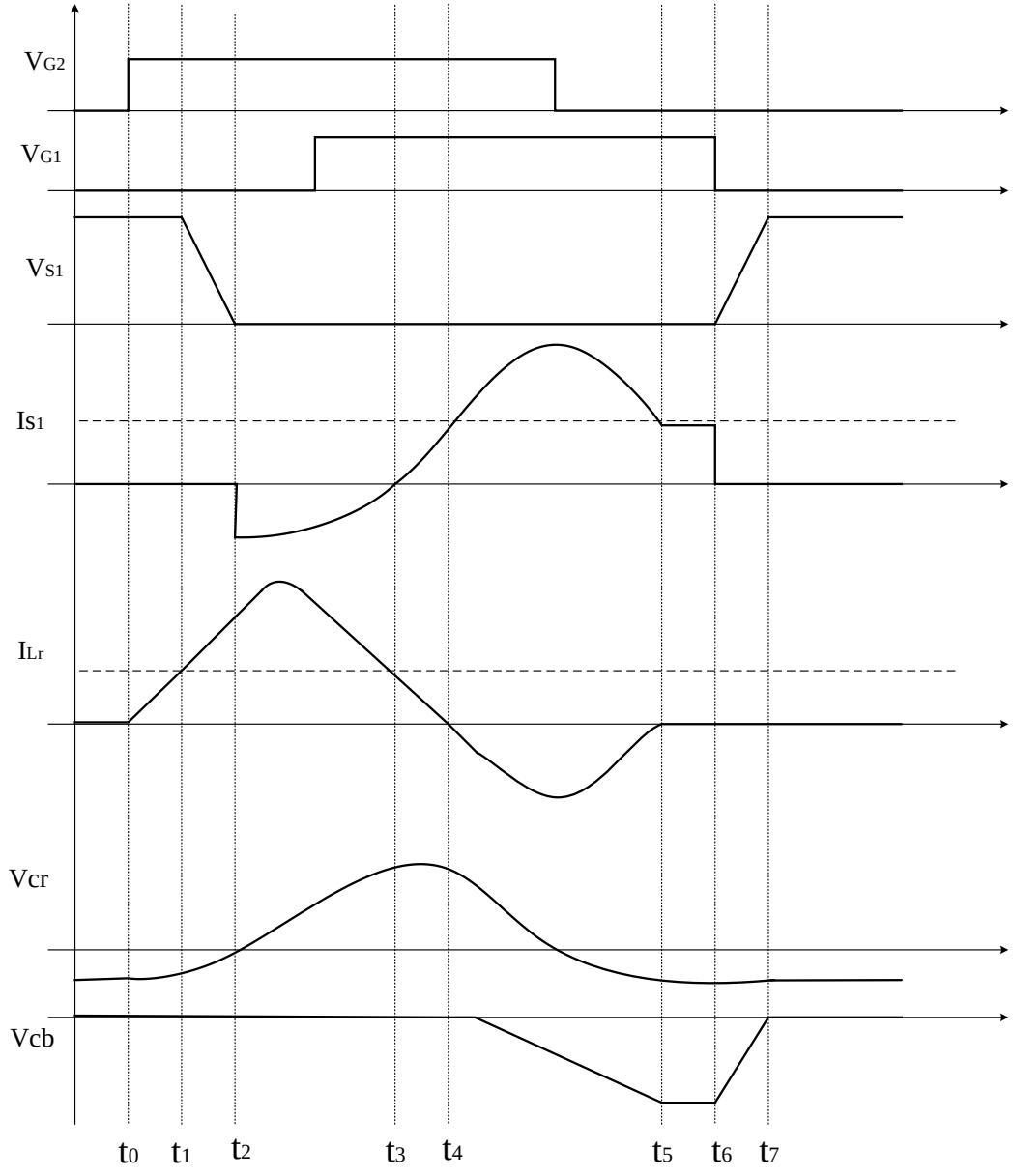

Figure 3.10: Hypothetical waveforms of the converter

It is to be noted that the resonant cycle (The time during which the auxiliary circuit supplements the main circuit) is just a small part of the entire switching cycle. For easy understanding the operation in resonant cycle is more focused on. The simple boost converter operation interval i.e. [t_5-t_6] is time compressed. Only that part of the waveform is compressed in which there will be no change in the waveforms, or the variables remains constant.

For further detailing in the ZVS turn ON of the S_1, all the waveforms are put together on common time axis and shown. Figure 3.11 shows the zero voltage interval during which the main switch has to be turned ON. The waveforms of current carried by the resonant inductor, voltage blocked by the resonant capacitor, voltage blocked by the feed forward capacitor and the main switch voltage are overlapped for easy understanding.

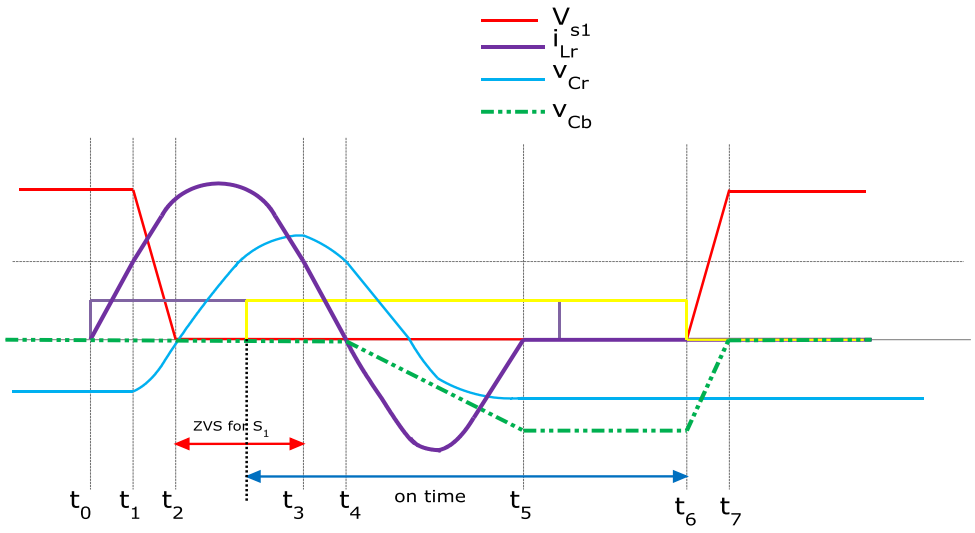

Figure 3.11: ZVS interval for S_1

3.4 CONVERTER DESIGN

Design objectives:

The converter is designed to meet the following objectives:

1. Minimize the switching losses the main switch.
2. Minimize the turn-off losses the main switch.
3. Reduce the EMI of the boost diode.
4. The auxiliary circuit resonant cycle must be kept as short as possible because with the increase in the cycle length the losses in the auxiliary circuit increase.

Design specifications:

The specifications for the design of the converter are given in table 3.1. The specifications include converter output power rating, input voltage range, output voltage, allowable ripple percentage in current and voltage etc.

Sl.No.	Parameter	Specification	Value
1	Output power	P_{0ut}	250W
2	Output voltage	V_{0ut}	400V
3	Input voltage	V_{in}	90-265V
4	Switching frequency	F_{sw}	100kHz
5	Output voltage ripple	V_{rp}	1%
6	Input current peak ripple	ΔI_{rpp}	20%

Table 3.1 Converter specifications for design

DESIGN PROCEDURE

The design procedure of this converter is divided into two parts:

I. Design of the boost or power circuit which is active for entire switching cycle.
II. Design of the auxiliary resonant circuit which is active for a resonant cycle which is just a minor part of the switching cycle.

3.4.1 DESIGN OF POWER CIRCUIT

The power circuit consists of the main switch, boost diode, input inductor and the output capacitor. Calculation of each circuit element values is shown very clearly.

Input inductor L_{in}:

The numerical value of the input inductor L_{in} , must be decided first because its value sets the peak input current which the converter switches have to withstand and therefore this current is necessary to decide the rating of other power circuit components. The maximum current without ripple is

$$I_{in\_pk} = \frac{\sqrt{2}\,\frac{P_{0ut}}{\eta}}{V_{in}} = \frac{\sqrt{2}\cdot\frac{250}{0.95}}{90} = 4.135A \tag{3.1}$$

The maximum peak-peak ripple current is

$$\Delta I_{rpp} = I_{pk\_\max}\cdot\Delta I = 4.135\times 20\% = 0.827A \tag{3.2}$$

Therefore the maximum peak input current with ripple is

$$I_{rpk\_\max} = I_{pk\_\max} + \frac{\Delta I_{rpp}}{2} = 4.135 + \frac{0.827}{2} = 4.55A \tag{3.3}$$

The duty ratio of the converter when the maximum current occurs is

$$D_{pk} = 1 - \frac{\sqrt{2}\cdot V_{in\_\min}}{V_0} = 1 - \frac{\sqrt{2}\cdot 90}{400} = 0.682 \tag{3.4}$$

The input inductor value is calculated as follows

$$L_{in} = \frac{\sqrt{2}\cdot V_{in\_\min}\cdot D_{pk}}{\Delta I_{rpp}\cdot F_{sw}} = \frac{\sqrt{2}\cdot 90\cdot 0.682}{0.827\cdot 100kHz} = 1050\mu H \tag{3.5}$$

Where F_{sw} is the switching frequency

Output capacitor:

The output capacitor acts as an energy storage element. It stores energy when the input voltage and current are near their peak and provides this energy to the output load when the line is low. The point of reference for selection of this capacitor is the endurable ripple in the output voltage. The peak charging current of the capacitor is

$$I_{chg\_pk} = \frac{P_{0ut}}{V_{0ut}} = \frac{250}{400} = 0.625A \tag{3.6}$$

The voltage ripple across C_0 is

$$V_{chg\_pk} = \frac{I_{chg\_pk}}{2 \cdot \pi \cdot f_r \cdot C_0}$$

$$C_0 = \frac{I_{chg\_pk}}{2 \cdot \pi \cdot f_r \cdot V_{chg\_pk}} = \frac{0.625}{2 \cdot \pi \cdot 120Hz \cdot (0.01 \cdot 400)} = 207\mu F \tag{3.7}$$

Boost diode:

The maximum voltage across the boost diode will be the output voltage V_0=400V which appears across the diode when the main switch remains in the conducting state. The peak current that flows through the diode is the peak with ripple of the current flowing through boost inductor i.e. $I_{rpk\_\max} = 4.55A$. The average current flowing through the diode is

$$I_{D1\_avg} = \frac{P_0}{V_0} = \frac{250}{400} = 0.625A \tag{3.8}$$

The peak current rating of the main boost switch depends upon the auxiliary circuit. So it is designed after the auxiliary circuit.

3.4.2 DESIGN OF THE AUXILIARY CIRCUIT AND MAIN SWITCH

Base values:

The base voltage is defined as:

$$V_b = V_0 = 400V \tag{3.9}$$

The base current is defined as:

$$I_b = I_{pk\_\max} - \frac{\Delta I_{rpp}}{2} = 4.135 - \frac{0.827}{2} = 3.722 \tag{3.10}$$

Therefore the base impedance is defined as:

$$Z_{rb} = \frac{V_b}{I_b} = \frac{400}{3.722} = 107.48\Omega \tag{3.11}$$

The base time is defined as the natural resonant cycle of the auxiliary circuit and is given as:

$$T_r = 2 \cdot \pi \cdot \sqrt{L_r \cdot C_r} \tag{3.12}$$

The worst case condition is where the ZVS interval will be least which occurs when the input boost current is at its maximum peak. At this value of peak current the impedance Z_{rb} will be 1 p.u. and the auxiliary circuit has to be designed for this value only.

Resonant Inductor L_r:

The selection of the inductor L_r is made keeping in mind that the D_1's reverse recovery current is to be made zero. Therefore selection of resonant inductor depends on the boost diode's turn-off di/dt and this can be controlled by slowly rerouting the current flowing through it to resonant inductor.

With increase in the value of the inductor the rise time of the current flowing through it increases which in turn decreases the reverse recovery current of D_1. But this increases the resonant cycle T_r, which results in an increase of ohmic losses due to increase in the rms currents of the auxiliary circuit. So a compromise must be made in the selection of resonant inductor.

L_r is chosen such that it lets the auxiliary current to increase up to the input peak current I_{in_pk} within 3 times the reverse recovery time t_{rr} of D_1 that is specified.

The boost diode must be an ultra-fast recovery diode with as low value of t_{rr} as possible as a slower diode requires a larger value of L_r. So an ultra-fast diode which will satisfy all voltage and current requirements and have minimum t_{rr} is selected. Assuming the value of t_{rr}=30ns the value of L_r can be calculated as follows

$$L_r = \frac{3 \cdot t_{rr} \cdot V_{s2\_pk}}{I_b} = \frac{3 \cdot 30ns \cdot (0.7 \cdot 400)}{3.722} = 5.8\mu H \cong 6\mu H \tag{3.13}$$

Where V_{s2_pk} is the peak voltage that appears across S_2 and is assumed 0.7 pu [1].

Resonant Capacitor C_r:

The value of resonant capacitor C_r is selected from the graph of ZVS interval vs. resonant impedance Z_r. We have to choose C_r that will give adequate ZVS turn-on interval as well as good turn-off. For proper design we select the curve K=3 and Z_r=0.21 pu [1] and the value of C_r can be determined as follows

$$Z_r = \sqrt{\frac{L_r}{C_r}} \Rightarrow C_r = \frac{L_r}{Z_r^{\,2}}$$
$$Z_r = Z_{r\_pu} * Z_{rb} = 0.21 \times 107.469 = 22.568\Omega \therefore C_r = 11nF \tag{3.14}$$

Auxiliary capacitor C_b:

ZVS at turn-off is provided by capacitor C_b. the selection of this capacitor is easy and is as follows

$$K = \frac{C_r}{C_b} = 3$$
$$C_b = \frac{C_r}{K} = 3.66nF \tag{3.15}$$

Rating of the auxiliary switch:

From the values of K and Z_r chosen it is found that the peak voltage blocked by auxiliary switch V_{s2_pk} is found to be

$$V_{s2\_pk} = 0.64pu \times 400V = 256V \tag{3.16}$$

The peak current flowing through the switch is found to be

$$I_{s2\_pk} = 1.61pu. \times 3.722 = 5.99A \tag{3.17}$$

The rms current of the switch is found to be

$$I_{s2\_rms} = (I_{ss2\_rms}, pu) \cdot I_b \cdot \sqrt{T_r \cdot F_{sw}} = (0.53) \cdot 3.722 \cdot \sqrt{1.58\mu s \cdot 100kHz} = 0.786A \tag{3.18}$$

Rating of the auxiliary circuit diodes:

The auxiliary circuit diodes have the same voltage rating as that of boost diode. The two series diodes D_2 and D_4 will conduct the same peak current as auxiliary switch S_2. The peak current carried by diode D_5 is also somewhat same as the above. The peak current carried by diode D_3 is the peak current with ripple I_{rpk_max} that flows in the converter was found to be 4.55A. The average current through diode D_2 is found to be

$$I_{D2\_avg} = (I_{D2\_avg}, pu) \cdot I_b \cdot T_r \cdot F_{sw} = (0.21pu) \cdot (3.722A) \cdot 1.587\mu s \cdot 100kHz = 0.12A \tag{3.19}$$

Rating of the main switch:

The maximum voltage that this switch must be able to handle is the output voltage V_0 with ripple. The ripple present in the output voltage can be found as

$$V_{chg\_pk} = 0.01 \times 400 = 4V \tag{3.20}$$

Thus the switch S_1 must handle 404 volts

The peak current carried by the main switch is $2.27\,pu \times 3.722 = 8.448A$ (3.21)

The maximum rms current for the switch is found to be

$$I_{s1\_rms} = I_{pk\_\max} \cdot \sqrt{\frac{1}{2} - \frac{4 \cdot V_{in\_\min} \cdot \sqrt{2}}{3 \cdot \pi \cdot V_0}} = 3.722 \cdot \sqrt{\frac{1}{2} - \frac{4 \cdot 90 \cdot \sqrt{2}}{3 \cdot \pi \cdot 400}} = 2.25A \quad (3.22)$$

The voltage across the capacitor C_b for K=3 and Z_r=0.21 is -0.87 pu. This means that the voltage blocked by switch S_1 during turn-off is 0.13 pu. Therefore voltage blocked by switch S_1 is found to be

$$0.13pu \times 400 = 52V$$

Therefore the turn-off losses are also greatly reduced.

3.5 SIMULATION OF THE CONVERTER

The converter circuit shown in figure-1 is simulated in MATLAB simulink environment by taking the component values shown in table 3.2.

Sl.no.	Circuit component	Symbol	specification
1	Resonant inductor	L_r	6µH
2	Resonant capacitor	C_r	15Nf
3	Feed-forward capacitor	C_b	3.5Nf
4	Boost inductor	L_{in}	1050µH
5	Output capacitor	C_0	470µF
6	Input voltage	V_{in}	265V
7	Switching frequency	F_{sw}	100kHz

Table 3.2 Component specifications for simulation

CHAPTER-4

PHOTOVOLTAIC ARRAY MODELLING

4.1 INTRODUCTION

A Photovoltaic system plies solar modules or panels for converting solar energy to electrical energy. The basic unit of a PV array is a PV cell.

4.1.1 PHOTOVOLTAIC CELL

This is similar to simple P-N junction devices. When sunlight hits the surface of the PV cell, the photons are absorbed by the atoms in the semiconductor material and electrons are freed from the negative layer. When this cell is connected to an external circuit, the free electrons find a path to reach the positive layer. The current generation process is shown in figure 4.1

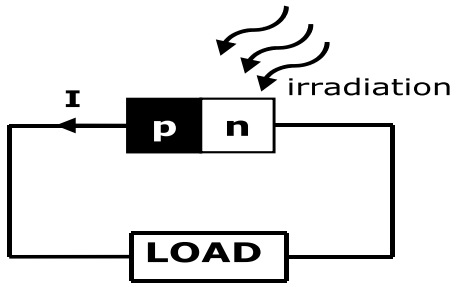

Figure 4.1 photocurrent generation

Detailed construction and working of a PV Cell:

PV cells are usually manufactured from various types of semiconductor materials using disparate processes. In present days, the monocrystalline and polycrystalline are mostly found. Si cells have a Si film that is connected to terminals of other devices. One side of the layer undergoes a process of addition of impurities, usually called doping to materialize a P-N junction. A very thin grid (metallic) is planted on the top of the PV cell which faces the sun.

As the light is incident on the surface of the cell, charge carriers are generated, which originates an electric current when the cell becomes a part of a loop or is connected to a load. As the energy of the incident photon becomes sufficient to break the covalent bond and detach the electrons of the semiconductor, charge carriers are generated. Photons that have lower energies than the energy gap of PV cell are not of any use and they help generating no voltage. Whereas Photons that have energy surpassing the band gap can produce electricity, but the energy associated with the band gap is only made use of. The remaining energy will be dissipated in the form of heat [10].

4.1.2 PHOTOVOLTAIC MODULE

The voltage generated by a single cell is very low around 0.5 volts. So a number of cells should be connected in serial and parallel to achieve the desired output. Diodes may be needed in order to avoid reverse current in the array, in case of partial shading.

4.1.3 PHOTOVOLTAIC ARRAY

The power generated by a single module may not be sufficient to supply the most of the appliances. So a group of modules are connected in series which is generally used for high voltage applications and in the same way they are connected in parallel, the connection which is useful for high current applications.

4.2 MODELING OF PV SYSTEM

4.2.1 PV CELL MODELING

The single diode model of a single PV cell is manifested in the figure 4.2. It includes a current source, a diode, parallel connected to the current source which represents the photocurrent, a series resistance R_s and a parallel resistance R_{sh}.

An accurate single diode model is depicted in the above figure. Equation 3.1 represents the current generated from the cell.

$$I = I_{PV} - I_0\left[\exp\left(\frac{V + IR_S}{aV_T}\right) - 1\right] - \left(\frac{V + IR_S}{R_P}\right) \tag{4.1}$$

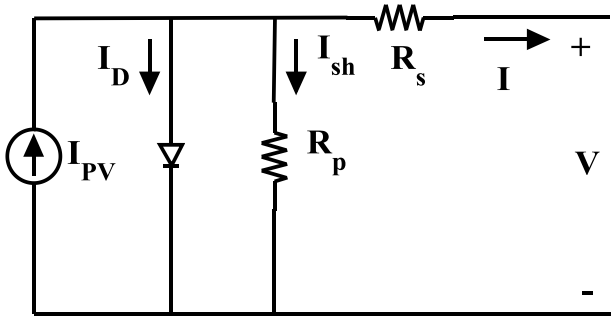

Figure 4.2 Analytical circuit of a practical PV cell

Where

I_0 is the diode's reverse saturation current

V_T is the diode's thermal voltage

a is the ideality factor of the diode

The equation of a PV current as a concomitant of changing environmental conditions, the temperature and irradiance can be written as

$$I_{PV} = \left(I_{PV\_STC} + K_I \Delta T\right)\frac{G}{G_{STC}} \tag{4.2}$$

Where

I_{PV_STC} is the photocurrent under Standard Test Conditions (STC)

$\Delta T = T - T_{STC}$ (in Kelvin) and T_{STC}=25°C

G is the irradiance on the surface of the cell

G_{STC} is the irradiance under STC (1000W/m²)

K_I is the short circuit current coefficient (generally provided by the manufacturer)

The equation for the saturation current of the diode is given as

$$I_0 = I_{0\_STC}\left(\frac{T_{STC}}{T}\right)^3 \exp\left[\frac{qE_g}{ak}\left(\frac{1}{T_{STC}} - \frac{1}{T}\right)\right] \tag{4.3}$$

Where

E_g is the energy gap of the semiconductor

I_{0_STC} is the nominal saturation current

The reverse saturation current equation can be further improved as a function of temperature as follows

$$I_0 = \frac{\left(I_{SC\_STC} + K_I \Delta T\right)}{\exp\left[\left(V_{OC\_STC} + K_V \Delta T\right)/aV_T\right] - 1} \tag{4.4}$$

Where

K_V is the temperature coefficient of open circuit voltage

I_{SC_STC} is the nominal short circuit current

V_{OC_STC} is the nominal open circuit voltage

4.2.2 PV ARRAY MODELING

All the above equations are applicable for a single PV cell. But in a typical installation of a PV power station, PV modules are used in which series and parallel connected PV cells are used in order to bridge the supply demand gap. Series combination of the cells increases the voltage and the parallel combination of the cells increases the current of the entire module

In such case, the output equation can be written as follows

$$I = I_{PV}N_P - I_0 N_P\left[\exp\left(\frac{V + IR_S\left(\frac{N_S}{N_P}\right)}{aV_T N_S}\right) - 1\right] - \left(\frac{V + IR_S\left(\frac{N_S}{N_P}\right)}{R_P\left(\frac{N_S}{N_P}\right)}\right) \tag{4.5}$$

The configuration of modules in a series parallel structure is shown in figure 4.3.

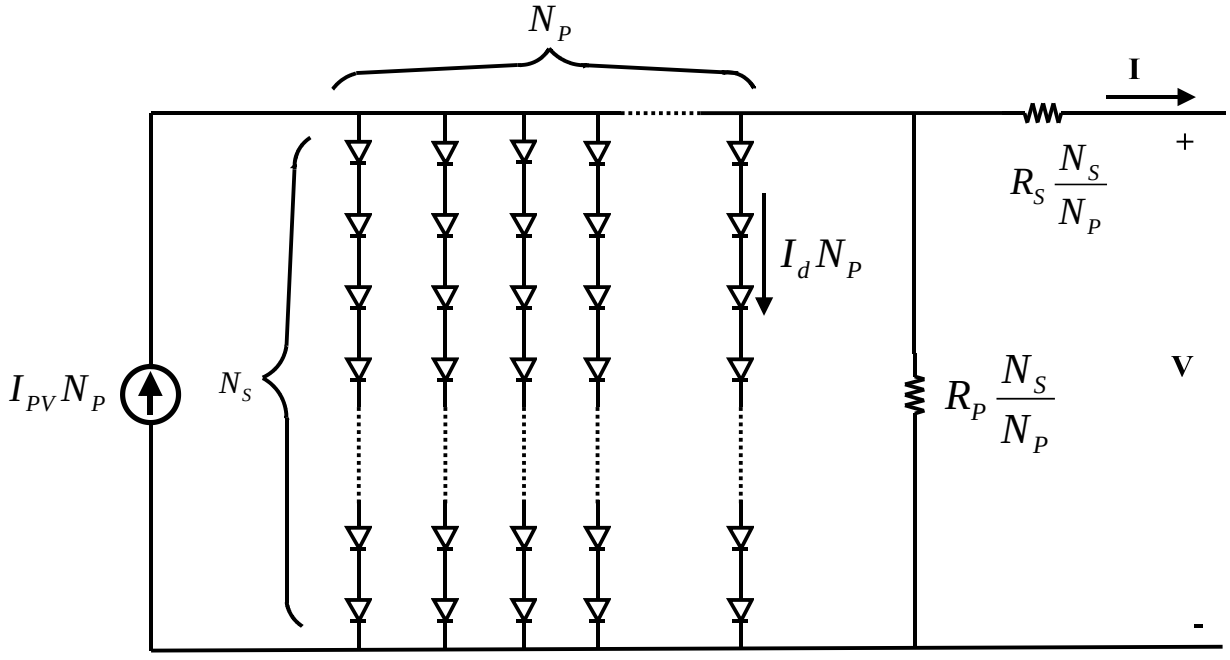

Figure 4.3: PV Module- representation of series parallel combination

The typical characteristics of a PV energy system are shown in the figures below. The Photovoltaic characteristics include the current voltage (I-V) characteristics and the power voltage (P-V) characteristics. The typical curves of these characteristics are shown. The point P_{max} in the I-V curve shows the point at which maximum power can be coerced. It represents the voltage at the maximum power point from the curve. This maximum power point is tracked from the P-V curve using different tracking techniques.

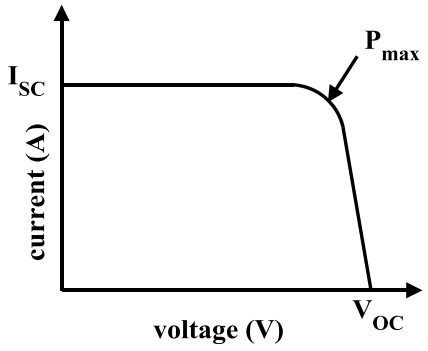

Figure 4.4: Typical I-V curve

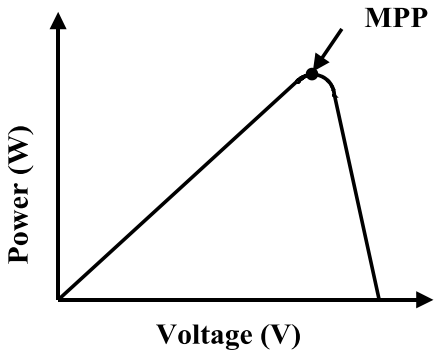

Figure 4.5: Typical P-V curve

The peak point of the P-V curve gives the maximum power point of a PV cell. This point will be different for different cells. But the maximum power point tracking system tracks the MPP of the system on a whole, i.e. all the cells connected. Recently research is going on implementing MPP tracking devices for each cell.

4.3 PV ARRAY SIMULATION

The PV module model is simulated in MATLAB simulink using the above equations. The parameters used for simulating the PV module are as shown in the table 4.1

Sl.No.	PARAMETER	SYMBOL	VALUE
1	Current at maximum power	I_{mp}	7.61 A
2	Voltage at maximum power	V_{mp}	26.3 V
3	Short circuit current	I_{sc}	8.21 A
4	Maximum power	P_{max}	200.143 W
5	Open circuit voltage	V_{oc}	32.9 V
6	Temperature coefficient of V	K_v	-0.1230 V/K
7	Temperature coefficient of I	K_i	0.0032 A/K

Table 4.1 Parameters of the simulated PV module

When a single module is simulated, the open circuit voltage of the module is found to be around 30 volts. But this voltage is found not to be present within the input voltage range of the designed converter. This voltage cannot be fed to the converter to check its operation in the PV environment. So 6 modules of similar kind are connected in serial so that the output voltage increases. When 6 modules are serial connected, then the output voltage of the array is raised to almost 180 volts. This voltage of 180 volts is within the input range of the designed Zero Voltage Transition DC-DC boost converter which is 90-265 volts.

CHAPTER-5

MAXIMUM POWER POINT TRACKING

5.1 INTRODUCTION

As the PV panel has non linear characteristics of voltage and current, MPPT algorithms are required to improve the efficiency of the PV system by setting the operating point to MPP of the characteristic curve. The only 3 major components of the PV energy system are the PV panels, the converter and the MPP tracker. The efficiency improvement of the first two components is that easy as it depends on the technology used and it may involve lot of cost. So the efficiency of the entire PV system can be improved cost-effectively by using MPPT algorithms [10].

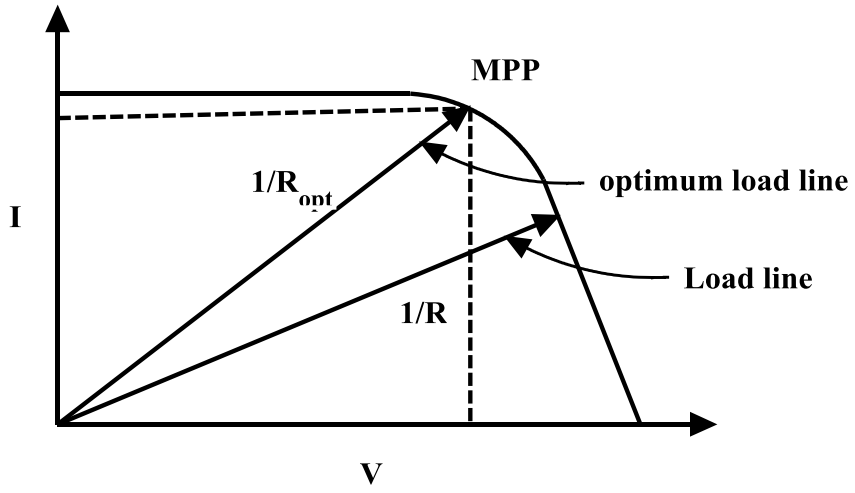

Fig 5.1: Concept of maximum power point tracking

Maximum power point (MPP) is an operating point on either IV or PV characteristic curve of a PV array. It is that point of operation, where the power supplied to the load is maximum. From maximum power transfer theorem, when the load of the converter is fixed and the duty cycle of the converter is varied which in turns varies the effective load on the PV

system, maximum power can be coerced from the PV energy system. In this way changing the slope of the load line and shifting the operating point and fixing it at the MPP, maximum power can be coerced from the PV array. The concept of maximum power point tracking is shown in figure 5.1

5.2 TYPES OF MPPT TECHNIQUES/ALGORITHMS

In recent years, many algorithms have been introduced to track maximum power point. They differ from one another in aspects like complexity, efficiency and cost. Some of them are

1. Perturb and observe
2. Incremental conductance
3. Fuzzy logic control
4. Neural networks
5. Fractional open circuit voltage
6. Fractional short circuit current
7. Current sweep
8. Maximum power point current and voltage computation
9. State based MPP tracking technique

From all the above techniques, we use Perturb and observe algorithm for simplicity.

5.3 PERTURB AND OBSERVE ALGORITHM

The Perturb and Observe algorithm is a kind of hill climbing technique. In hill-climbing, the duty cycle of the converter is perturbed and in P&O the DC link operating voltage or the voltage at the PV panel output or the converter input terminals is perturbed.

In this technique, the present perturbation is decided by the signs of the previous perturbations and increments. If the power is incremented by the last perturbation, then the perturbation should be in the same direction, where as if it results in the decrement of power, the

direction of the perturbation should be changed. The perturbations are repeatedly carried out until the MPP is attained.

5.4 FLOW CHART

The flow chart for the MPPT algorithm using P&O method is shown below in figure 5.2

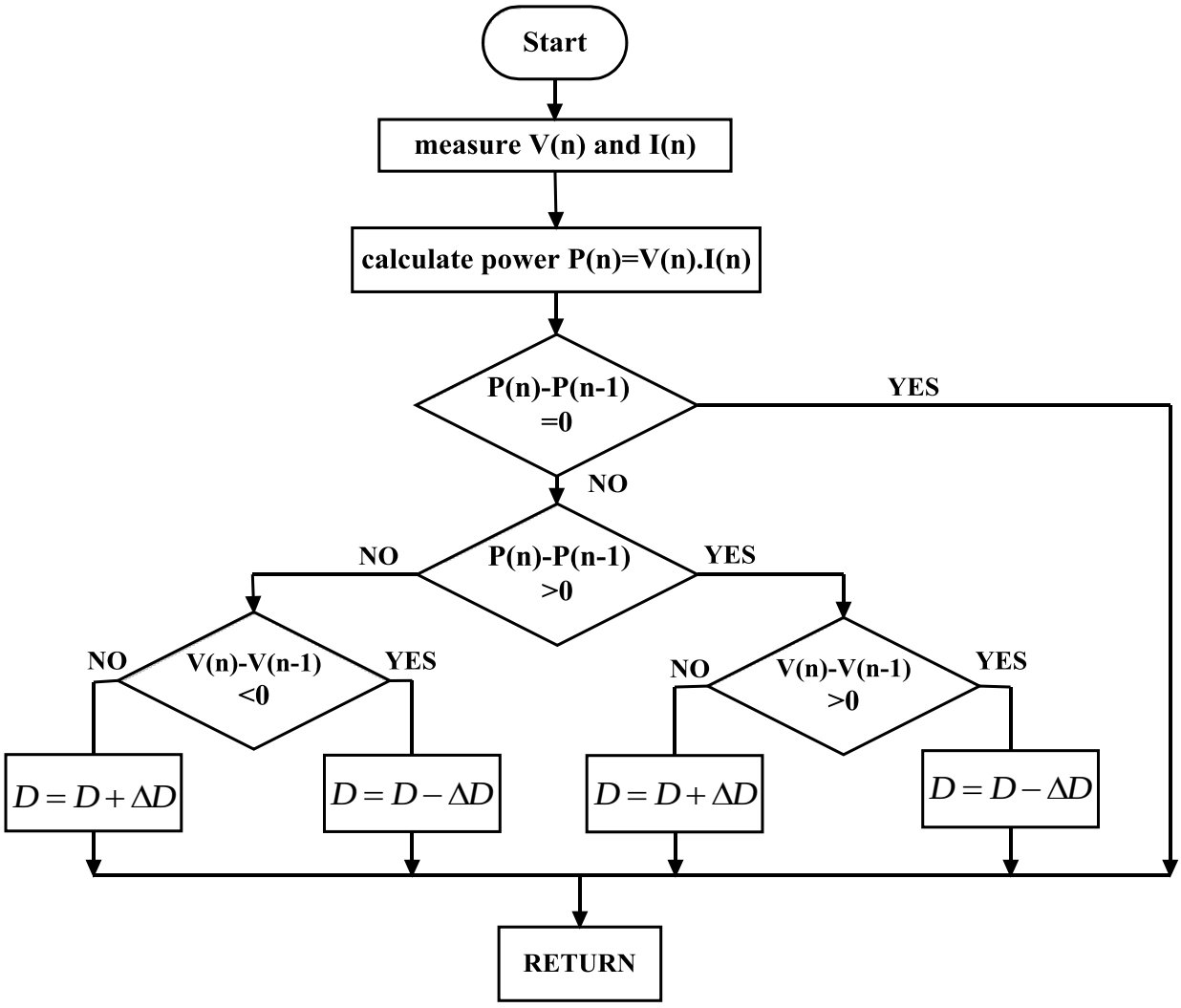

Fig 5.2: Flow chart for MPPT P&O algorithm

CHAPTER-6

RESULTS AND DISCUSSION

6.1 SIMULATION RESULTS OF CONVERTER

The operation of the converter is verified and the waveforms of the auxiliary circuit elements for a resonant cycle and the main switch current and voltage waveforms for one switching cycle are shown below.

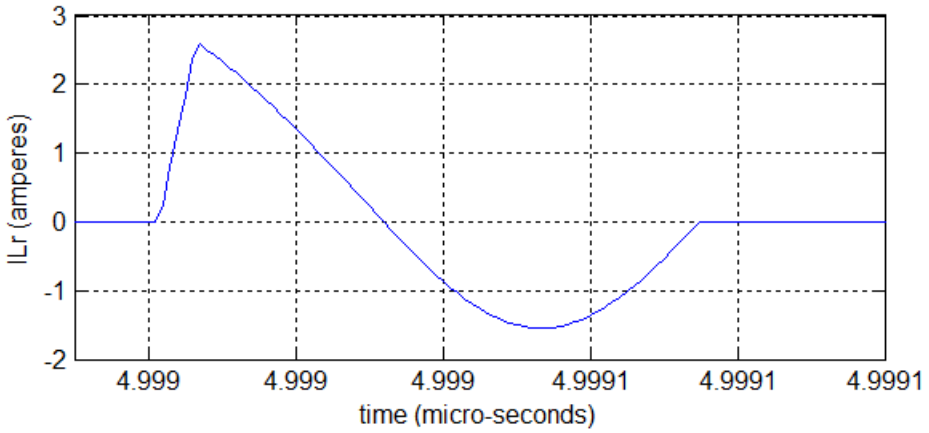

Fig 6.1: Auxiliary inductor current

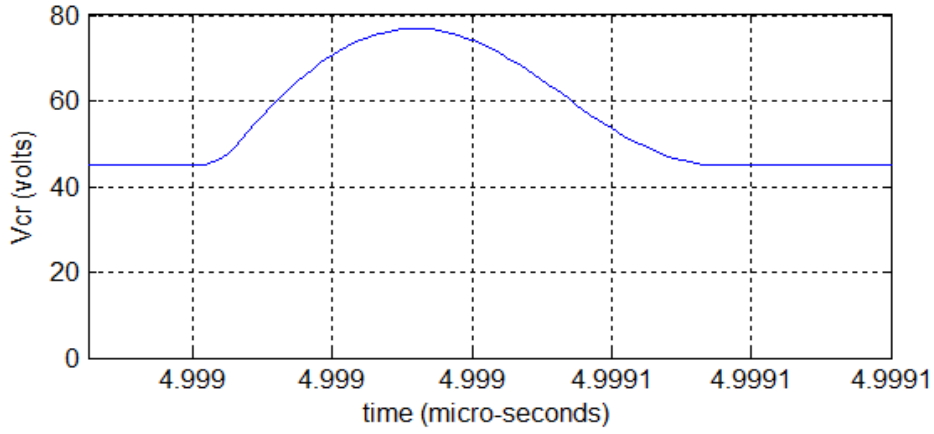

Fig 6.2: Auxiliary capacitor voltage

Figures 6.1 and 6.2 show the resonating circuit waveforms for one resonant cycle which is a part of the switching cycle. These waveforms are compared with the analytical waveforms shown in the figure 3.10. Figure 6.3 shows the feed forward capacitor voltage waveform.

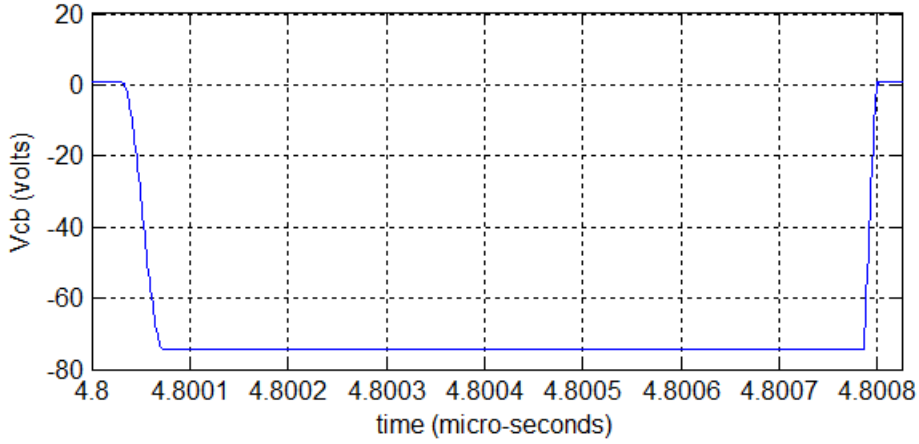

Fig 6.3: Feed-forward capacitor voltage

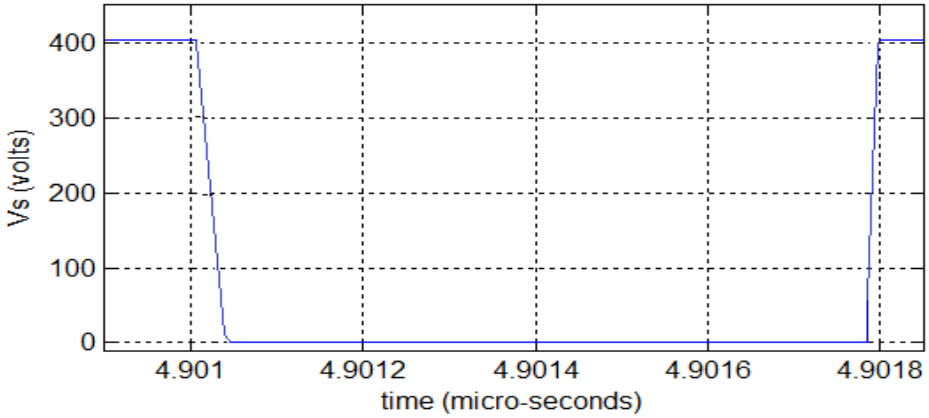

Fig 6.4: Main switch voltage

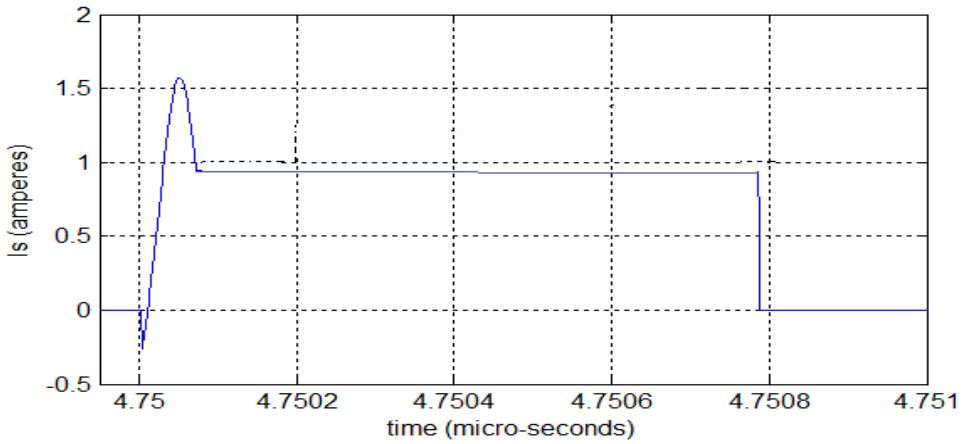

Fig 6.5: Main switch current

Figure 6.4 manifests the main switch voltage waveform and the figure 6.5 shows the main switch current waveform. Superimposing one on the other, the zero voltage turn ON of the main switch is manifested in figure 6.6 and the reduced voltage turn-off of the main switch is manifested in figure 6.7. The voltage during turn-OFF is measured to be 80 volts.

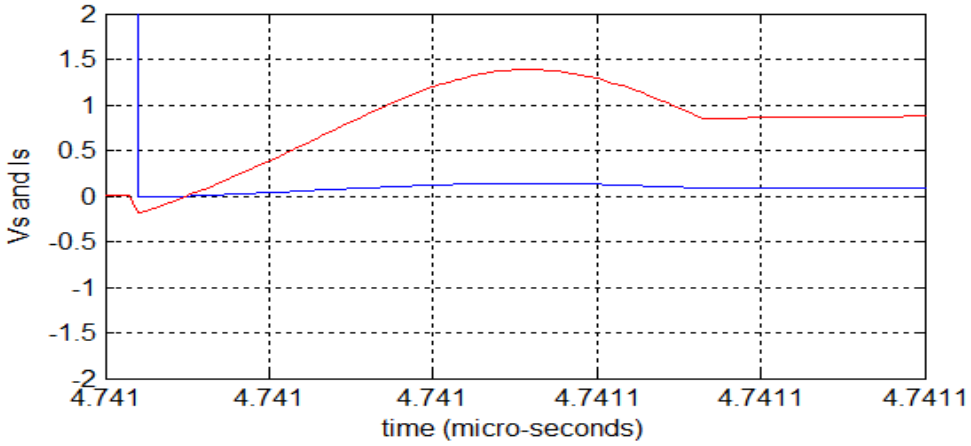

Fig 6.6: ZVS turn ON of S_1

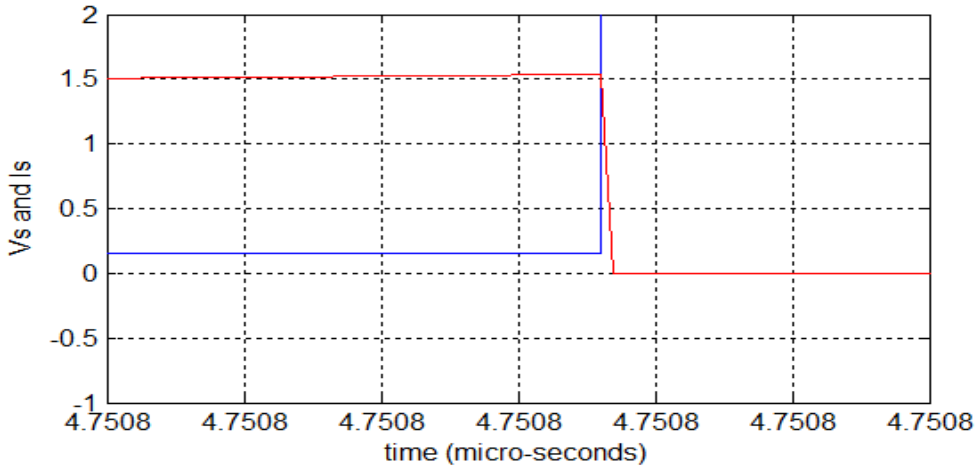

Fig 6.7: Reduced voltage turn OFF of S_1

The switching transitions of the auxiliary switch S_2 ZCS turn-ON and the ZVS turn-OFF are shown in the figures 5.8 and 5.9 respectively.

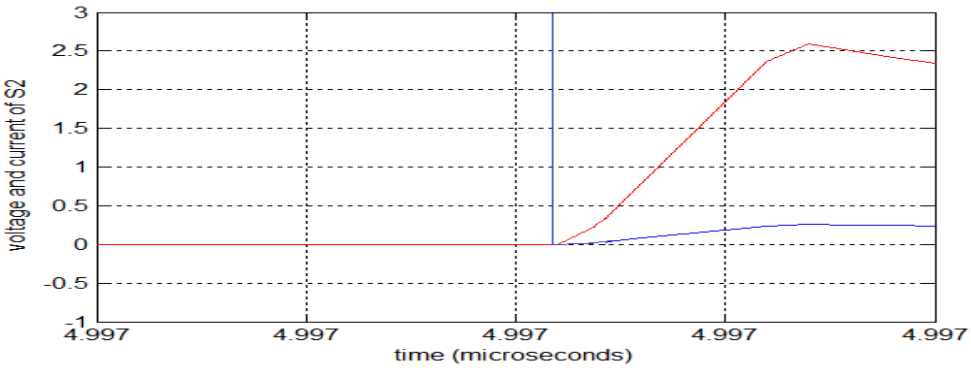

Fig 6.8: ZCS turn ON of S_2

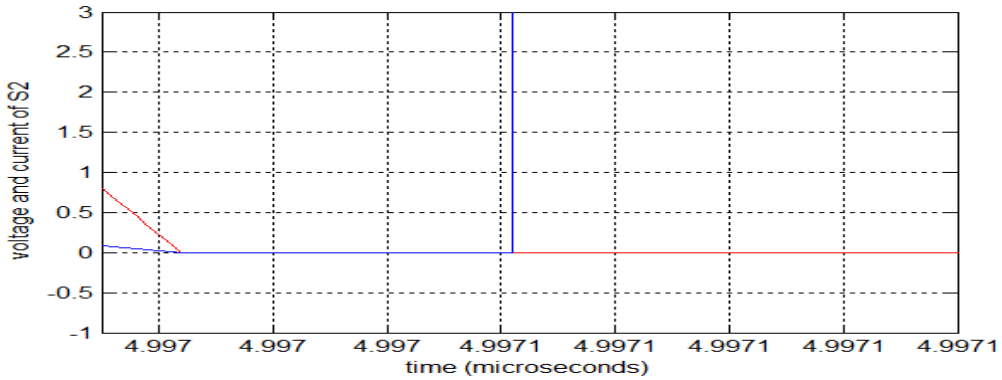

Fig 6.9: ZVS turn OFF of S_2

The circuit is run under different input conditions with input voltage ranging from 100-265V and the circuit is found to give an output voltage of 400V for different values of duty cycles ranging from 35-81.2% and is shown in table 6.1.

Input voltage V_{in}(V)	Duty cycle δ (%)	Input voltage V_{in}(V)	Duty cycle δ (%)
265	35.00	185	56.45
260	36.25	180	57.80
255	37.60	175	59.25
250	38.90	170	60.70
245	40.20	165	62.10
240	41.60	160	63.60
235	42.85	155	65.10
230	44.20	150	66.54
225	45.56	145	68.10
220	46.90	140	69.70
215	48.30	135	71.3
210	49.60	130	73
205	51.00	125	74.7
200	52.30	120	76.6
195	53.70	115	78.65
190	55.00	110	81.2

Table 6.1 Duty cycle corresponding to input voltage for 400V output

Also the RMS current flowing through the auxiliary switch is measured for different values of input voltage and is tabulated below in table 04

Input voltage (volts)	Duty cycle (%)	Rms current of switch-2(Amps)
265	35.00	0.135
200	52.30	0.243
150	66.54	0.415
110	81.20	0.634

Table 6.2 RMS current of auxiliary switch

6.2 LOSS CALCULATION AND COMPARATIVE STUDY

In order to carry out the comparative study, a conventional hard switching converter is designed for the same specifications. A boost converter with the component values given in table 6.1 is simulated and the losses of both the converters are compared.

Sl.No.	Component	Symbol	Value
1	Boost inductor	L_{in}	5.58mH
2	Output capacitor	C_o	1.21μF

Table 6.3 components for conventional hard switching converter

The switching losses of any switch is calculated using the following formula

$$P_{sw} = V_0 \cdot I_0 \cdot F_{sw} \cdot \left(\frac{T_{on} + T_{off}}{2} \right) \tag{6.1}$$

6.2.1 LOSSES IN THE STUDIED SOFT SWITCHING CONVERTER

The main switch's turn ON transition takes place under zero voltage. Therefore from the above formula the switching losses of the main switch during turn ON are zero.

$$P_{sw1on} = 0W$$

The main switch's turn OFF transition takes place at reduced voltage and the voltage during turn OFF is measured and is found to be 80V and the peak current that is carried by this switch is measured to be 4A.

The switching losses during turn OFF time is calculated as follows

$$P_{sw1off} = 80 \cdot 4 \cdot 10^5 \cdot \left(\frac{0 + 100 \times 10^{-9}}{2} \right) = 1.6W$$

The auxiliary switch's turn ON transition takes place under ZCS and its turn OFF transition takes place under ZVS. Therefore the switching losses of S_2 are zero.

$$P_{sw2on} = P_{sw2off} = 0W$$

The total switching losses are

$$P_{sw} = P_{sw1} + P_{sw2} = 1.6 + 0 = 1.6W$$

The conduction losses of the switches are calculated using the formula

$$P_{sw\_cond} = 1.8 \cdot I_{s\_rms}{}^{2} \cdot R_{on} \qquad (6.2)$$

The rms current of the main switch is measured to be 2.3481Amperes and the conduction losses are calculated as follows

$$P_{cond\_s1} = 1.8 \cdot 2.3481^{2} \cdot 0.85 = 8.4357W$$

The rms current of the auxiliary switch is measured to be 0.786 Amperes and the conduction losses are calculated as follows

$$P_{cond\_s2} = 1.8 \cdot 0.786^{2} \cdot 0.85 = 0.947W$$

The total conduction losses of the switches are

$$P_{cond\_s} = 8.4357 + 0.947 = 9.3827W$$

The conduction losses of the diode are product of the forward voltage drop across the diode and the average current flowing through it. The forward voltage drop is measured to be 0.8027 Volts and the current flowing through it is the load current which is 0.625 Amperes. So the conduction losses of the diode are calculated as follows.

$$P_{D\_cond} = V_F \cdot I_{D\_avg} = 0.8027 \cdot 0.625 = 0.5016 \cong 0.502W$$

The total losses in the converter are

$$P_{losses} = P_{sw} + P_{cond} + P_D = 1.6 + 9.3827 + 0.502 = 11.4847W$$

The efficiency of the converter is calculated as follows

$$\eta = \left(\frac{P_0}{P_0 + P_{losses}} \right) \times 100 = \left(\frac{250}{250 + 11.484} \right) \times 100 = 95.6\%$$

6.2.2 LOSSES IN CONVENTIONAL HARD SWITCHING CONVERTER

The only switch in this converter is hard switched and the switching losses are calculated using the equation 6.1. The voltage across the switch during ON and OFF conditions is 400V and the peak current is measured to be 4.6A. The switching losses of the switch in conventional boost converter are

$$P_{sw} = 400 \cdot 4.6 \cdot 10^5 \cdot \left(\frac{100 \times 10^{-9} + 100 \times 10^{-9}}{2} \right) = 18.4W$$

The conduction losses in the hard switching converter are calculated using the formula given in equation 6.2. The rms current flowing through the switch is measured to be 2.2632A. The conduction losses are calculated as

$$P_{sw\_cond} = 1.8 \cdot 2.2632^2 \cdot 0.85 = 7.836W$$

The conduction losses of the diode remain same as that of the soft switching converter.

$$P_{D\_cond} = V_F \cdot I_{D\_avg} = 0.8027 \cdot 0.625 = 0.5016 \cong 0.502W$$

The total losses in the converter are

$$P_{losses} = P_{sw} + P_{cond} + P_{D\_cond} = 18.4 + 7.386 + 0.502 = 26.288W$$

The efficiency of the converter is calculated as follows

$$\eta = \left(\frac{P_0}{P_0 + P_{losses}} \right) \times 100 = \left(\frac{250}{250 + 26.288} \right) \times 100 = 90.4\%$$

All the results obtained from the comparative study are tabulated and shown in table 6.2

Sl.No.	Specification	Hard switching converter	Soft switching converter
1	P_{sw}	18.4	1.6
2	P_{cond}	7.386	9.3827
3	P_D	0.502	0.502
4	%η	90.4	95.6

Table 6.4

6.3 SIMULATION RESULTS OF PV ARRAY

The simulation results of the PV array are shown below. The IV characteristics and PV characteristics are in figures 6.10 and 6.11 respectively. The open circuit voltage of the simulated PV array is 180 volts and the short circuit current is 2.25 amperes.

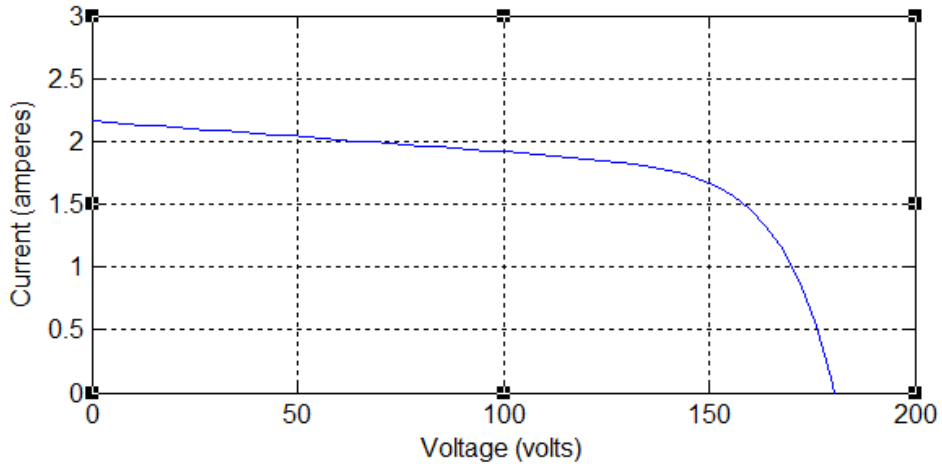

Fig 6.10: IV characteristics of the PV array

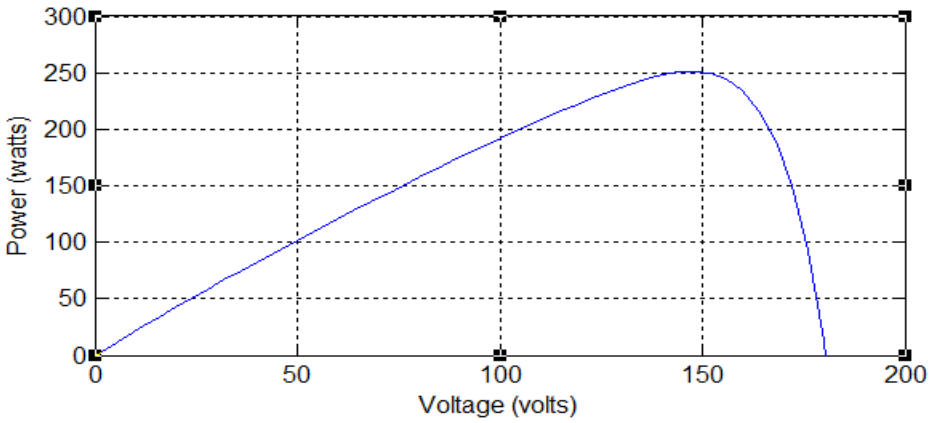

Fig 6.11: PV characteristics of the PV array

The tracked operating point at which maximum power can be extracted using an MPPT algorithm is shown below in figure 6.12

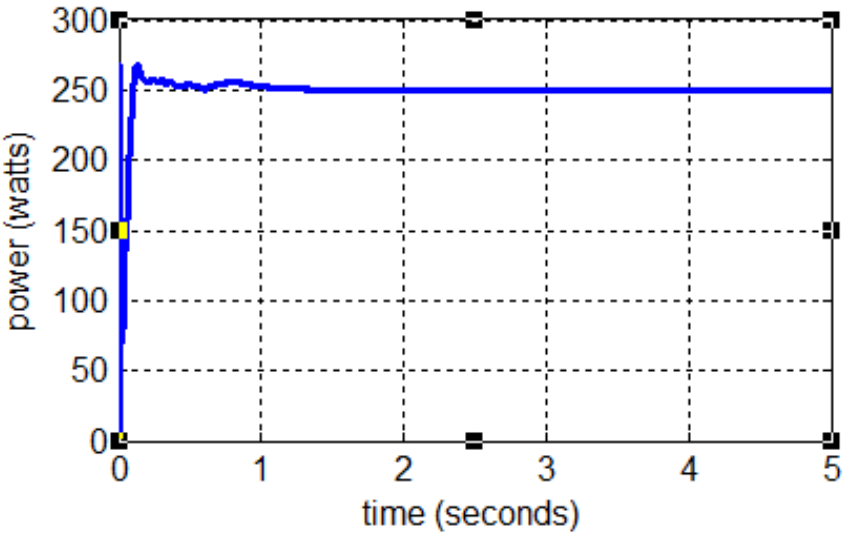

Fig 6.12: Output power of the PV array after MPPT

6.4 CONCLUSIONS

- The main switch losses of conventional converter are much greater than those of the soft-switched converter.
- The auxiliary switch losses are zero in both converters since no auxiliary switch in conventional converter and in the new converter it is soft switched.
- The diode conduction losses remain same in both the cases
- The conduction losses vary by the RMS current carried by the switches. It is found to be more in soft switched converter since the auxiliary circuit losses are added up to conduction losses.

But the switching loss contribution of the hard switching converter dominates in the calculation of total losses and hence the soft-switched converter is found to be more efficient than the conventional hard-switched converters.

6.5 FUTURE SCOPE

Work may be done on further reducing the voltage during turn-off transition of the main switch or making it zero without increasing the circuit complexity.

REFERENCES

[1] Nikhil Jain, Praveen K.Jain and Geza Joos, "A Zero Voltage Transition Boost Converter Employing a Soft Switching Auxiliay Circuit With Reduced Conduction Losses," in *IEEE Transactions on power electronics*, vol.19, no.1, January 2004.

[2] In-beom Song, Doo-yong Jung, Young-hyok Ji, Seong-chon Choi, Yong-chae Jung and Chung-yuen Won, "A Soft Switching Boost Converter using an Auxiliary Resonant Circuit for a PV System," *International Conference on Power Electronics - ECCE Asia* May 30-June 3, 2011.

[3] Basu S., Undeland T.M., "Diode recovery characteristics considerations for optimizing EMI performance of continuous mode PFC converters," *Power Electronics and Applications, 2005 European Conference, pp.9 pp.,P.9, doi: 10.1109/EPE.2005.219496*.

[4] John Bazinet and John A.O'Connor, "Analysis and Design of a Zero Voltage Transition Power Factor Correction Circuit," Unitode Integrated Circuits Merrimack, NH 03054.

[5] G.Moschopoulos, P.Jain, Y.Liu and Geza Joos, "A Zero Voltage Switched PWM Boost Converter with an Energy Feedforward Auxiliary Circuit," *IEEE Transactions on Power Electronics*, vol.14, paper 653-662, July 1999.

[6] Sang-Hoon Park, Gil-Ro Cha, Yong-Chae Jung and Chung-Yuen Won, "Design and Application fro PV Generation System Using a Soft-Switching Boost Converter with SARC," *IEEE Transactions on Industrial Electronics*, vol.57, no.2, February 2010.

[7] Saravana Selvan. D, "Modeling and Simulation of Incremental Conductance MPPT Algorithm for Photovoltaic Applications," *International Journal of Scientific Engineering and Technology*, Vol.2, no.7, paper no: 681-685, July 2013.

[8] M G Villalva, J R Gazoli and E R Filho, " Comprehensive Approach to Modeling and Simulation of PV Arrays," *IEEE Transactions on Power Electronics*, vol.24, no.5, May 2009.

[9] T Salmi, M Bouzguenda, A Gastli and A Masmoudi, "Matlab/Simulink based Modeling of solar Photovoltaic cell," *International Journal of Renewable Energy Research*, vol.2, no.2, 2012.

[10] David Sanz Morales, "Maximum power point tracking algorithms for PV applications," *student paper, Alto university*.

[11] J. Surya Kumari, Dr. Ch. Sai Babu, A. Kamalakar babu, "Design and analysis of P&O and IP&O MPPT techniques for PV system," *International Journal of Modern Engineering research*, vol.2, issue.4, paper 2174-2180, July-Aug. 2012.

[12] Salam Z., Ishaque K. and Taheri H., "An improved two-diode photovoltaic (PV) model for PV system," *Power Electronics, Drives and Energy Systems (PEDES) & 2010 Power India, 2010 Joint International Conference*, vol., no., pp.1,5, 20-23 December 2010.

[13] S. Sheik Mohammed, "Modeling and Simulation of Photovoltaic module using MATLAB/Simulink," *International Journal of Chemical and Environmental Engineering*, Vol.2, No.5, October 2011.

[14] Jenifer A., N. R. Newlin, G. Rohini, and V. Jamuna, "Development of Matlab Simulink model for photovoltaic arrays," *International Conference on Computing, Electronics and Electrical Technologies (ICCEET), 2012*, pp. 436-442. IEEE, 2012.

[15] Ismail Aksoy, Haci Bodur, and A. Faruk Bakan, "A New ZVT-ZCT-PWM DC–DC Converter," *IEEE transactions on power electronics*, Vol. 25, N0. 8, August 2010.

[16] Aryuanto Soetedjo, Abraham Lomi, Yusuf Ismail Nakhoda, Awan Uji Krismanto, "Modeling of Maximum Power Point Tracking Controller for Solar Power System," *TELKOMNIKA (Indonesian Journal of Electrical Engineering*), Vol.10, No.3, pp. 419-430, July 2012.